


## Performance evaluation of asphalt binder modified with lignin-derived nanocarbon

Mirtes Aila de Carvalho Brasil<sup>1</sup>, Leni Figueiredo Mathias Leite<sup>1</sup>, Francisco Thiago Sacramento Aragão<sup>1</sup> ,  
Patrícia Hennig Osmari<sup>2</sup>, Luiz Silvino Chinelatto Júnior<sup>3</sup>, Luis Alberto Herrmann do Nascimento<sup>3</sup>,  
Margareth Carvalho Coutinho Cravo<sup>3</sup>, Joyce Rodrigues de Araujo<sup>4</sup>

<sup>1</sup>Universidade Federal do Rio de Janeiro, Programa de Pós-Graduação em Engenharia Civil. Rio de Janeiro, RJ, Brasil.

<sup>2</sup>Universidade de São Paulo, Departamento de Engenharia de Transportes. São Carlos, SP, Brasil.

<sup>3</sup>Petrobras, Centro de Pesquisas, Desenvolvimento e Inovação Leopoldo Américo Miguez de Mello. Rio de Janeiro, RJ, Brasil.

<sup>4</sup>Instituto Nacional de Metrologia, Qualidade e Tecnologia. Duque de Caxias, RJ, Brasil.

e-mail: mirtes.brasil@coc.ufrj.br, lenimathias@coc.ufrj.br, fthiago@coc.ufrj.br, patriciahosmari@usp.br, lsil-vino@petrobras.com.br, luisnascimen-to@petrobras.com.br, cravo@petrobras.com.br, jraraujo@inmetro.gov.br

### ABSTRACT

This paper evaluates the mechanical behavior of nanocarbon modified asphalt binder. The nanocarbon was produced by a pyrolysis process of lignin. Three samples of asphalt binder were used as base for modification, a Pen 30/45, a Pen 50/70, and a SBS-polymer-modified 55/75. Different conditions of temperature, stirring speed, and modification time periods were evaluated to identify the best operational conditions. The characterization of nanocarbon was performed by different methodologies. Performance tests were conducted in a dynamic shear rheometer (DSR) to determine dynamic shear modulus, phase angle, and parameters of the Linear Amplitude Sweep test (LAS) and Multiple Stress Creep and Recovery test (MSCR) on the modified and unmodified asphalt samples. Furthermore, tests were performed in a bending beam rheometer (BBR) to measure the flexural creep stiffness and *m*-value at low temperatures, as well as the  $\Delta T_c$  parameter. The samples were submitted to short- and long-term aging, and then master curves were constructed from frequency sweep dynamical shear tests. The results indicated that small amounts (0.02% to 0.05%, w/w) of nanocarbon adopted in the research were enough to improve rutting, fatigue, and aging resistance. Finally, the results also revealed that the modified asphalt 55/75 was better homogenized with the nanocarbon than the neat asphalt cements 30/45 and 50/70.

**Keywords:** Nanocarbon, aging, asphalt binder, fatigue, rutting.

### 1. INTRODUCTION AND THEORETICAL BACKGROUND

The demand for modified asphalts around the globe has increased in the recent years as a consequence of the growing traffic volumes in asphalt pavements. In addition, there is the need to improve connecting routes between locations and to facilitate the transportation of people and goods.

At the end of last century, the modified asphalts began to be applied in flexible pavements of Brazilian Concessions, using micro surfacing or hot mixes. The first modifiers in Brazil were the copolymers styrene-butadiene-styrene (SBS) and random styrene-butadiene rubber SBR. In the last two decades, asphalt rubber terminal blend has been used in chip seals, dense hot mixes, and gap graded mixes. The reactive terpolymer has been also used in dense mixes or chip seals. The research centers and the academia are constantly investigating and developing new materials as modifiers, especially sustainable products.

The demand for new sustainable products has resulted in the recent growth of research in the development of graphene materials from lignin [1]. Being a byproduct of the pulp and paper industry and having an estimated worldwide production of more than 70 million tons per year [1], the conversion of lignin onto carbon nanomaterials has become an increasingly attractive possibility.

Fatigue cracking is a traffic-related phenomenon and one of the major distresses observed in the Brazilian highways. It is also aging-related [2] and has motivated researchers to develop advanced characterization techniques to understand and predict its cumbersome material failure mechanisms. On the other hand, rutting

occurs mostly in the first Summer after the wearing course construction, due to high traffic volume, especially in urban roads and highways.

The goal when adopting modifiers is to achieve superior performance and durability. In addition to the conventional modifiers available in the market, alternative products have been evaluated, including residual plastics, ground tire rubber, polymerized vegetal oils, and tall oil derivatives.

Graphene is a thin layer carbon material that has become a research hot topic in the recent years due to its excellent thermal conductivity, mechanical strength, electron mobility, and surface area. These outstanding properties encourage the application of graphene in various fields [3]. For instance, graphene-like materials have been employed as asphalt binder modifying agents in pavement engineering. It has been reported in the literature that the graphene-modified asphalt binders (GMABs) exhibit an enhanced performance grade, a lower thermal susceptibility, a higher fatigue life, and a decreased accumulation of permanent deformations in comparison to an unmodified binder [4]. Graphene-based materials present excellent mechanical, thermal, and physical properties, allowing them to be good candidates for application in modified asphalt production. Several studies have been reported in the field of modified asphalt using graphene-based materials, such as flake graphite (FG), graphene nanoplatelets GNPs, functionalized graphene sheets, and graphene oxide (GO), with promising results and enhanced performance of the modified asphalt [5].

ASIMN *et al.* [5] summarized different nanocarbon products that were blended with asphalt binder using amounts in the range of 0,1 to 7% wt./wt. at temperatures from 120°C to 160°C with shear stirring from 100 rpm to 400 rpm. These data came from different papers published between 2017 and 2021. The modified asphalts obtained using these operational conditions presented enhanced aging characteristics, rutting and fatigue performance. HE *et al.* [6] also presented a synopsis from different studies using graphene, GNPs, and GO blended with asphalt binder. Different mixing parameters were employed: manual shear stirring and mechanical stirring of 5000 rpm, temperature range of 135°C to 190°C, and mixing periods between 10 minutes and 120 minutes. According to MORENO-NAVARRO *et al.* [7], the graphene addition could reduce the asphalt phase angle. Higher graphene contents may lead to phase angle reductions of 10%. On the other hand, the asphalt elastic properties and the thermal conductivity could be improved.

Lignin is a phenolic macromolecule with a complex, heterogeneous, three-dimensional, high-carbon structure, and is the second most abundant sustainable natural polymer on the planet. It is the main source of aromatics in nature, once it is present in the vegetable cell walls [8]. This raw material is capable of producing carbon nanomaterials with characteristics like those obtained from graphite, yet with low cost and low environmental impact. Research has demonstrated that it can be used in asphalt paving, providing improvements to the binder mechanical behavior.

Graphene, GNPs, and GO have the potential to improve the performance of the asphalt mixture. The asphalt mixture stability can be effectively improved through the introduction of GO due to the presence of lipophilic (oxygenated) groups to the dense network structure of the asphalt binder, already modified by copolymer styrene-butadiene-styrene (SBS) [9].

HAN *et al.* [10] presented several methodologies for mixing graphite and its derivatives to the asphalt binder. In the specific case of GO, the modifier contents ranged between 0.02% and 3% in different asphalt binders, namely Pen 70, Pen 90, and modified by SBS [10]. The operating mixing conditions were agitation in the range of 4000 rpm and temperatures from 135°C to 170°C. The asphalts modified by nanocarbon products were analyzed by infrared spectrophotometry. It was observed that the modification results were due to the different physical mixing configurations and the chemical reaction, since the GO layered structure with large surface area facilitates the uniformization and complete mixing with the macromolecular structure of the asphalt binder. This contributes with the improvement of the mechanical and rheological properties of the modified binder. It was also found that the GO oxygenated functional groups can form hydrogen bonds with asphalt components, in addition to attracting each other via Van der Waals forces [10].

The lignin treatment steps consisted of ultraviolet light radiation exposure followed by a hydrothermal carbonization in autoclave, vacuum degassing, and subsequent pyrolysis, proceeded by the final ultrasound exfoliation of the material recovered from the previous steps. The lignin-derived nanocarbon (LNC) was generated with a sp<sup>2</sup>-hybridized nano porous framework structure with oxygenated functional groups attached. The characterization of the lignin-derived nanocarbon was carried out using X-ray diffraction measurements, infrared, Raman and X-ray photoelectrons spectroscopies analyses [11].

The oxygenated functional groups present the advantage to allow the nanocarbon modifier to be reactive and compatible with many polymer matrices. Literature review shows that considerably small amounts of nanocarbon (0.1% to 0.2%) are enough to improve rutting characteristics [12]. This research demonstrated that the addition of up to 0.2% in mass of GO (nanocarbon oxygenated) enhance the high-temperature elasticity and

rutting resistance of non-modified/SBS modified binders. The performance improvements were attributed to an increase in the crosslinking degree of the binders induced by the GO. The GO amount required to improve the high-temperature performance of the nonmodified binder was smaller than the amount required for the SBS modified binder [13]. The results of Fourier-transform infrared spectroscopy (FTIR) indicated that the incorporation of GO inhibited the deterioration of the asphalt binder and reduced the degradation of the SBS modifier during the thermo-oxidative aging and photo-oxidative aging processes. Also, the thermogravimetry analysis (TGA) test results indicated that the GO powder could improve the SBS thermal stability [14].

LNC shows similarities with graphene, GNPs, and GO in terms of chemical composition and process production. It has been evaluated as an asphalt modifier in the last ten years, presenting good performance and a promising applicability potential.

The discovery of a new modifier with such characteristics originated from a sustainable source can be a great contribution to the academic community and to the industry. In that sense, the comprehensive characterization of such materials is a key step to evaluate if they behave similarly to the similar materials found in nature.

This study evaluates the resistance to rutting, fatigue, and aging of asphalt binders modified with lignin-derived nanocarbon, produced in laboratory, after an optimization of its operational conditions [11]. The research evaluates the potential improvement in binder performance provided by the incorporation of lignin-derived nanocarbon in terms of rutting, fatigue, and aging resistance. It also identifies the benefits of the lignin-derived nanocarbon on the 55/75 SBS-modified asphalt in comparison with other binders with higher SBS contents and supposedly better performances, i.e., a 60/85 and a 65/90.”

## 2. MATERIALS AND METHODS

### 2.1. Asphalt binders

The neat binders investigated in this research are classified as penetration grades 50/70 and 30/45, while the SBS-modified is a 55/75. They were named as AC1, AC2, and SBS, respectively. These materials were modified with different LNC contents and blended following various operational conditions. Rheological tests were carried out to evaluate the different blend performance and the material aging. Chemical tests were also performed for a better understanding of the LNC addition. The binder grades and production processes are presented in Table 1.

The evaluation of lignin-derived nano carbon as modifier of asphalt binder was performed based on the following rheological parameters:  $J_{nr}$  from Multiple Stress Creep and Recovery (MSCR) ASTM D 7405/20 [15], Fatigue Factor of the Binder (FFB) from Linear Amplitude Sweep (LAS) AASHTO T 391/20 [16], Delta Tc ( $\Delta T_c$ ) AASHTO PP 78/17 [17], German standard DIN 52050/18 [18], entitled “BTSV binder characterization rapid test” (bitumen typisierung schnell verfahren), GRP and R, and the South African T int parameter.

#### 2.1.1. Rutting index

Superpave continues to evolve in the search for parameters that properly characterize the behavior of binders when applied in the field. As an example, the current version of the specification, ASTM 8239-21 [19], requires the characterization of MSCR parameters to estimate the binder permanent deformation potential and indicate the proper traffic level that can be applied to the material in the field.

#### 2.1.2. Cracking indexes

LAS is a rheological test that is not included in the Superpave specification. Nevertheless, it has been regarded as a good fatigue predictor [20]. The continuum damage approach is adopted to calculate parameters obtained from rheological properties and amplitude sweep test results that are performed to infer the material resistance to fatigue. This method is intended to evaluate the ability of an asphalt binder to resist fatigue damage by employing cyclic loading at increasing amplitudes to accelerate the material damage [21].

Although threshold values for this test have not been consensually defined yet, several researchers have been performing LAS tests on different types of asphalt binders and accumulating comprehensive databases

**Table 1:** Binder properties.

ASPHALT BINDER	TRADITIONAL GRADE	PRODUCTION PROCESS	PG GRADE
AC 1	50/70	Vacuum residue	64S-22
AC 2	30/45	Vacuum residue	64H-16
SBS	55/75	SBS modified	64E-22

that can be potentially used soon to define such limiting criteria. A criterion was recently developed based on the relationship between LAS for binders and uniaxial fatigue for asphalt concrete mixtures, considering the simplified viscoelastic continuum damage theory (S-VECD). Underwood and Kim [22] proposed the so-called FFB based on the area below fatigue life curves between strain levels of 1.25% and 2.50%. This index, calculated with Equation 1, was named as FFB19°C, given that the tests were performed at 19°C [20]. Research has demonstrated that FFB is well correlated with the fatigue resistance of asphalt mixtures by means of direct tension testing results and with the pavement surface cracked area in the field [10].

$$FFB_B = \frac{(\log(N_{f,1.25\%}) + \log(N_{f,2.5\%}))}{2} \times (\log(0,025) - \log(0,0125)) \quad (1)$$

$\Delta T_c$  is another cracking parameter with a high potential to become a strong rheological index, given that it is easily calculated from the well-established Bending Beam Rheometer (BBR) test method, that has been adopted by Superpave to estimate the binder low PG temperature. The crude source of the asphalt binder is closely related to  $\Delta T_c$ , including the production process and modifier type [23]. Although  $\Delta T_c$  is a parameter developed to predict low-temperature failure and fatigue cracking is related to intermediate temperatures, both phenomena are linked to the stress relaxation potential of the binders [20]. The limits of  $\Delta T_c$  adopted by the majority of American Departments of Transportation (DOT) is -5°C. However, polymer-modified binders may present low  $\Delta T_c$  values, out of the allowed limits, even though they are typically less prone to cracking than unmodified binders. NCHRP 09-59 was recently published to disclose research efforts that aimed to identify fatigue-indicating binder properties in asphalt mixtures that can be used in asphalt binder specifications. For this purpose, 16 asphalt binders were tested in various fatigue-related tests, and the results were correlated and validated considering laboratory and field asphalt mixture test results, as well as traffic simulator results [24]. The results showed that the GRP parameter and the R value were the best indicators of binder fatigue, according to the criteria of correlation with performance, equipment cost, ease of implementation, and engineering robustness. GRP correlates better than the specification requirement  $|G^*| \sin \delta$ .

The critical issue on the  $|G^*| \sin \delta$  parameter is related to the determination of the adequate testing temperature rather than the parameter itself. Ideally, the fatigue test temperature should be linked to the intermediate pavement temperature, although the specification does not seem to determine it correctly. Thus, the authors decided to relate the fatigue test to the low pavement temperature.

GRP is measured at a frequency of 10 rad/s and at an intermediate temperature determined only by the low-temperature PG. A limit of 5 MPa has been proposed, similar to that of the existing AASHTO M320 [25] specification. This measurement can be made following the AASHTO T 315 [26] protocol on material aged in the pressure aging vessel (PAV) for 20 hours and is well correlated with fatigue cracking under controlled strain [24].

The R-value of the Christensen-Anderson model can be calculated from the creep stiffness and the relaxation rate (m-value) of the BBR test and correlates well with  $\Delta T_c$ . The proposed limit range is 1.5 to 2.5, after RTFOT and 20-hour PAV aging. Equation 2 is used to calculate the R-value. In the equation, S is the BBR creep stiffness at 60 seconds and m is the BBR relaxation rate at 60 seconds [24].

$$R = \log(2) \times \frac{\log\left(\frac{S}{3000}\right)}{\log(1-m)} \quad (2)$$

Where S (MPa) is the BBR creep stiffness at 60 seconds and m is the BBR relaxation rate at 60 seconds.

A long-term aging parameter does not exist in the Superpave specification. For that purpose, the South African performance specification includes the parameter  $|G^*|$  after RTFOT + PAV divided by the virgin  $|G^*|$  measured at an intermediate temperature ( $T_{int}$ ) that is determined by Equation 3 [27].

$$T_{int} = [(T_{max} + T_{min})/2 + 4]^\circ\text{C} \quad (3)$$

Where  $T_{max}$  and  $T_{min}$  are the high and the low PG temperature, respectively.

### 2.1.3. Classification indexes

The German standard DIN 52050/18 [18], entitled “BTSV binder characterization rapid test” (bitumen typisierung schnell verfahren), is a new method to classify the asphalt binders [28]. The goal is to replace the

softening point and penetration tests by the BTSV methodology. Initially, the iso-module temperature corresponding to a  $|G^*|$  of 15 kPa is determined when performing a temperature sweep at the frequency of 1.59 Hz. From this temperature, in the phase angle versus temperature curve, the phase angle is determined. The temperature provides an indication of the binder stiffness, and the phase angle may provide information on the modification degree of the material. Low phase angles are associated with a high modification degree, while high phase angles indicate a low degree of modification. The BTSV methodology also allows evaluating the binder aging degree. In general, the phase angle reduces as the temperature increases, following a linear trend.

Another strategy has been adopted by a British standard 900/21 [29] to characterize the binder long-term aging. It is based on the loss complex modulus at 15°C, 10 Hz, and different aging levels (virgin, short term, and long term) [29].

## 2.2. Lignin-derived nanocarbon preparation

A preparation methodology, recently developed by the Division of Metrology of Materials (Dimat) of the National Institute of Metrology of Materials, Quality, and Technology (INMETRO), produces lignin-derived nanocarbon (LNC) from lignin by pyrolysis. This method has some advantages among the existing ones. One of the advantages that stands out is that it does not use catalysts and solvents, with the exception of ascorbic acid (vitamin C) as a solvent, which implies a more environmentally friendly process when compared to other existing methodologies [11].

The lignin used as base material for LNC synthesis is the sigma-Aldrich alkaline (CAS number: 8068-05-1). A light and dark brown powder of high purity Kraft lignin is produced from natural lignin by alkaline extraction. This lignin used as base material for the synthesis of LNC has a T<sub>g</sub> value of 130°C, which could be considered indirect evidence of a high amount of hydrogen bonds as in wood lignin.

Regarded as a low-value material, lignin is commonly used as boiler fuel to generate heat and electricity and as a component in adhesives, cement, and drilling fluids for underwater oil wells [30, 31]. The development of the LNC was based on examining the pre-treatment of lignin with the intention of preserving its aromatic chain units and promoting its cross-linking during pyrolysis, with the expectation of substantially higher yields and final technological value of the material, thereby making it possible to promote technologically viable improvements in lignin processing.

In the study by [30], a new approach was developed to produce a nanostructured carbon material with potential for implementation in the technological processes of lignin transformation. The method used a one-component starting material sourced directly from biomass. Different consecutive treatment steps were combined for the sequential transformation of lignin, aiming at a decrease in the total energy required to produce the lignin-derived nanocarbon. Each stage of treatment has a specific objective. An initial ultraviolet irradiation was carried out, which induced the formation of free radicals with an instantaneous reaction that promotes crosslinking of the polymeric chains, and, as a result, a more compact surface structure is obtained. In the study, a hydrothermal carbonization was carried out in an autoclave, enhancing the polycondensation of the aromatic rings.

Afterwards, an integral conversion (surface and volume) of the polymeric lignin matrix into a nanostructured carbon and a formation of a structure in intercalated layers with a reasonable long range structural ordering within the layers was observed. Chemical spectroscopy and microscopy studies showed that the pretreatment steps were crucial to produce, after pyrolysis, the LNC phase composed of ordered structural domains with the apparent lamellar morphology of randomly oriented sheets of carbon. It was concluded that the resulting materials presented hybrid orbital Carbon atom  $sp^2$  domains with oxygenated groups, tending to the formation of a structure like reduced graphene oxide [30].

## 2.3. LNC characterization

The recently-developed LNC was evaluated in this study. It was submitted to thermal analysis, X-ray diffraction (XRD), nuclear magnetic resonance (NMR), and elemental analysis and compared to graphene, reduced graphene oxide, and graphene oxide results available in the literature to better classify it in the nanocarbon family.

### 2.3.1. Elemental Analysis

The LNC sample was analyzed for C, H, N, O, and S contents by means of combustion followed by chromatography using a CHNSO analyzer (Thermo Scientific Instruments Flash 2000 model).

### 2.3.2. Thermogravimetric analysis

Thermogravimetric (TGA) measures the change in the mass of a sample as a function of the temperature in a controlled atmosphere. Therefore, TGA measurements were carried out to characterize the thermal stability of

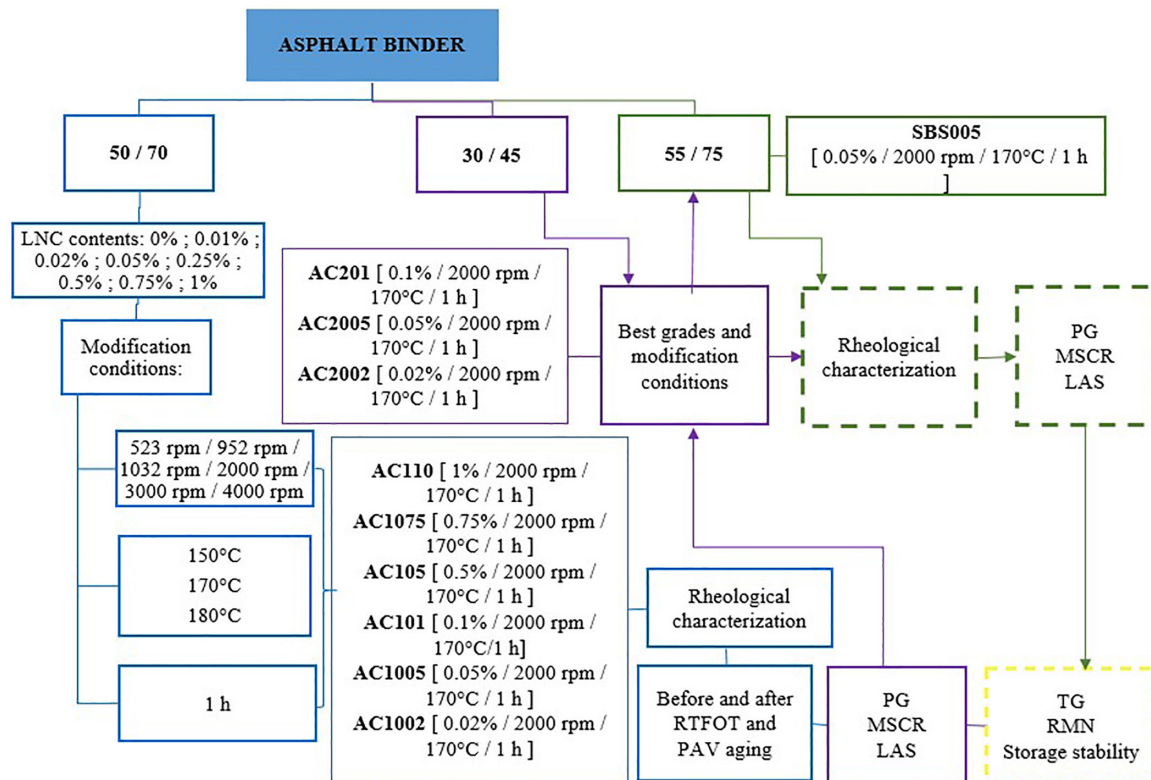


Figure 1: Experimental program.

the LNC sample and to provide a preliminary estimate of the sample composition. This technique is suitable to analyze materials that exhibit either mass loss or gain as a result of decomposition, oxidation, or loss of volatiles (such as moisture) within the investigated range of the temperature. The TGA tests were carried out in a TGA analyzer (TA Instruments SDTQ 600 model) in both N<sub>2</sub> (20°C – 700°C) and air (700°C – 1000°C) atmospheres. A heating rate of 20°C/min was adopted in both temperature ranges.

### 2.3.3. Solid-state nuclear magnetic resonance

Nuclear magnetic resonance (NMR) spectra were recorded in a Bruker Avance NEO 500 NMR spectrometer operating at 11.75 T (NMR frequency of 125.8 MHz for <sup>13</sup>C), at 25°C, using a solid-state NMR probe equipped with zirconia rotors (4 mm in diameter). Prior to the analyses, all samples passed through a #60 sieve (mesh opening of 0.25 mm) and were then packed into the rotors. The <sup>13</sup>C DP/MAS NMR spectra were recorded with <sup>13</sup>C pulse duration of 4.2 μs ( $\pi/2$  pulse), proton decoupling, with a 20.0 ms acquisition time, 4096 recorded transients, a 15 s recycle delay, and 12 kHz of MAS rate. The spectra were obtained by Fourier transform of the FIDs and were externally referenced by tetramethylsilane (TMS), using adamantane as a secondary reference ( $\delta(\text{CH}) = 37.8$  ppm and  $\delta(\text{CH}_2) = 28.7$  ppm).

### 2.4. Blending conditions

The research experimental plan was divided in stages, including determination of LNC content, mixing temperature, and speed. Initially, the blend preparation protocol considered different conditions for the 50/70 binder (AC1). This investigation was performed with the aim of optimizing the mixing conditions that ensure the best homogeneity and the lowest LNC content. Mixer rotation conditions and temperature were analyzed for each LNC content, slowly incorporated into the binder. Then, the optimized procedure was replicated for the other materials.

The selection of the blending conditions was based on the evaluation of various LNC contents, mixing temperature and rotation speed, as follows:

- LNC content: 0.01%, 0.02%, 0.05%, 0.1%, 0.25%, 0.5%, 0.75, and 1%. Similar contents were employed in different studies, such as [7, 13] and [14].

- Mixing temperature: 150°C, 170°C, and 180°C, also selected based on [7, 13], and [14].
- Mixing speed: 532 rpm, 1032 rpm, 2000 rpm, 3000 rpm, and 4000 rpm, tested for a mixing time of one hour.

The experimental program is summarized in the flowchart of Figure 1.

The optimal operational blending condition was determined considering the  $J_{nr}$  parameter. From the analysis, the best combination of temperature and stirring speed for the Pen 50/70 binder was identified. The optimal blending condition was temperature of 170°C and low shear stirring of 2000 rpm for one hour. As shown in Figure 2, lower LNC contents produced better rutting resistance, i.e., lower  $J_{nr}$  values. Such outcome led the study to employ low contents of LNC to prepare the blends. This condition was replicated for the Pen 30/45 and for the modified 55/75 binders.

### 2.5. Test methods used for LNC-modified asphalt

The experimental program comprised three steps, as follows. Each analysis was performed with at least two replicates.

- Characterization of the PG grade and rutting and fatigue resistance through MSCR and LAS tests, respectively, on PAV-aged samples.  $\Delta T_c$  and R were also determined from BBR results;
- Performance of frequency sweep tests with binder samples in different aging states, i.e., virgin, RTFOT-aged, RTFOT + PAV-aged to construct master curves and black spaces. From these curves, European rheological indexes, such as BTSV, RAI,  $|G^*|_{T_{int}}$ , and  $|G^*|$  at 10Hz and 15°C were determined;
- Identification of storage stability according to ASTM D 7173/21.

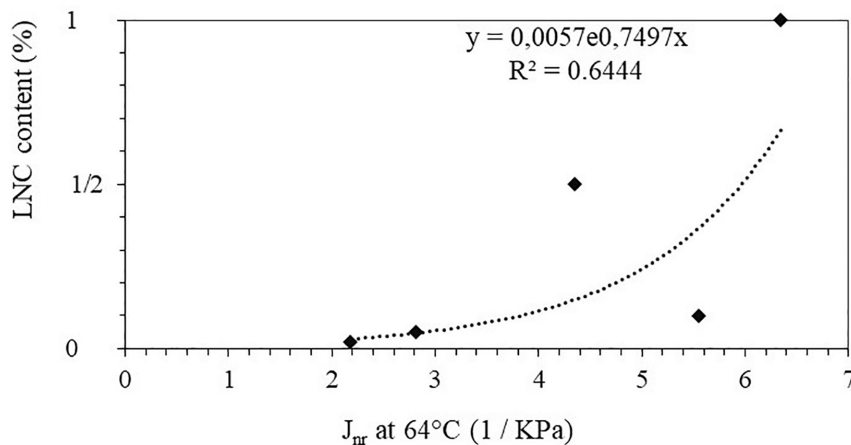


**Figure 2:** Effect of LNC content on rutting resistance.

Table 2 shows the contents and the designation of each modified asphalt binder.

**Table 2:** LNC contents and designations of the modified binders.

ORIGINAL BINDER	LNC CONTENT (%w/w)	DESIGNATION
AC1	0.5	AC105
AC1	0.75	AC1075
AC1	1.0	AC110
AC1	0.1	AC101
AC1	0.05	AC1005
AC1	0.02	AC1002
AC2	0.1	AC201
AC2	0.05	AC2005
AC2	0.02	AC2002
SBS	0.05	SBS05
SBS	0.02	SBS002

### 3. RESULTS AND DISCUSSION

This section presents the characterization of the LNC and of the LNC-modified asphalt, including Superpave PG grading, rutting resistance, fatigue resistance, aging susceptibility, effect of LNC addition in comparison with SBS-modified asphalt and stability storage.

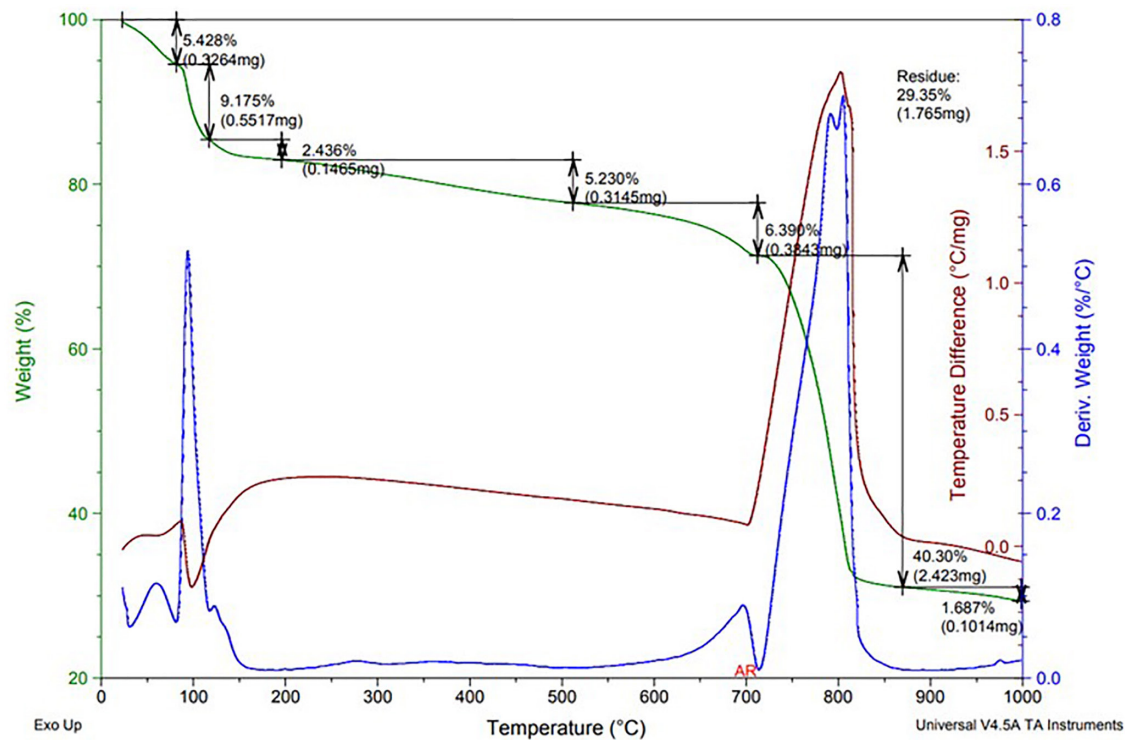
#### 3.1. LNC characterization

Table 3 presents the elemental analysis for the LNC, GO and RGO. The LNC sample presents low levels of S (0.3 wt%) and N (<0.3 wt%), and a high level of O (26,6 wt%). The results suggest the presence of about 20% of inorganic material in the LNC. Although not evaluated in the present work, dissolved metals such as Na and K should be present due to the alkaline extraction of lignin feedstock used for LNC production.

The results of TGA are presented in Figure 3, which depicts the weight loss curve thermogravimetric (TG) and derivative thermogravimetric (DTG) evolution profiles as a function of the reaction temperature for the LNC sample. The nearly 15% mass loss under 150°C could be attributed mainly to evaporation of physisorbed water naturally present in the material due the hydrophilic nature of its functional groups. A slight amount of light occluded species and/or entrained residual solvent (co-precipitant) used for the LNC production could be partially responsible for this mass loss. The mass loss around 400°C (near 5%) is probably a result of the removal of loosely bound oxygen containing functional groups. The partial thermal decomposition of the sample, attributed to the pyrolysis of more stable functional groups, is responsible for the appearance of a minor peak (close to 6%) around 600°C in the TGA thermogram.

**Table 3:** Elemental analysis of LNC in comparison with reduced graphene oxide and graphene oxide [31, 1].

ELEMENT CONTENT, % w/w	LNC	GO	RGO
Nitrogen	< 0.3	0 to 1	6
Carbon	51.2	61 to 68	37 to 85
Hydrogen	1.6	0 to 1	–
Sulfur	0.3	0 to 2	–
Oxygen	26.6	25 to 30	7 to 35



**Figure 3:** TGA results for the LNC.



It is noteworthy that naturally-present physiosorbed water will not harm the adhesion between aggregates and asphalt binder because it is not free water, but water molecules connected by intermolecular forces to carbon nanotube's structure. Furthermore, the quantities of LNC retrained in asphalt binder are very low.

After the introduction of air at 700°C, an exothermic weight loss is observed that can be attributed to the burning of aromatic core (40%). This corresponds to the air combustion of the high-molecular-weight compounds containing condensed rings. These results are in accordance with those usually reported in the literature for RGO from different origins. The ~29% mass left after 1000°C (slightly higher than the 20% predicted from elemental analyses) suggests that dissolved metals from lignin feedstock used for LNC production should be on its oxide form.

The lignin solid-state NMR spectrum represented in Figure 4 indicates the presence of typical constituting units, such as resonance lines near 56.8 ppm associated with methoxyl groups and signals between 105 and 155 ppm for aromatic carbons. The resonance lines due to aliphatic side chains in lignin can be seen between 8 ppm and 38 ppm. Small carbonyl signals arise in the region between 170 and 185 ppm.

The solid-state NMR spectrum for the LNC represented in Figure 4 indicates that the relative intensity of aromatic bands is much larger than that of the lignin groups in the natural sample. This infers the breakdown of methoxyl and aliphatic chain of lignin during LNC production. In comparison to the feedstock, the solid-state NMR of LNC shows a diminishment of the signals from oxygenated aromatic carbons (shoulder around 150 ppm). Finally, small peaks due to functional groups around 30 ppm and 80 ppm can be seen on the LNC solid-state NMR.

Overall, despite the nearly 29% mass of inorganic material, the LNC chemical composition is similar to the RGO chemical structure already reported in the literature [32]. For LNC, the effects of the presence of the delocalized  $\pi$  electrons should be pronounced as the material becomes structurally more ordered in aromatic planes arranged in graphite-like micro-crystallites. In fact, several electronic properties, such as electrical conductivity, magnetic susceptibility, and magnetoresistance are expected. These characteristics make LNC a good candidate for improving asphalt binder properties.

### 3.2. LNC modified asphalt analysis

#### 3.2.1. Superpave specification

The PG grade (ASTM D 8239/21) [33] and PG continuous grade of all samples (ASTM D 7643/22) [19] are presented in Table 4. The continuous grade temperatures and continuous grade may be used for forensic or research studies and when producing, blending, modifying, or otherwise evaluating asphalt binders. In general, PG the continuous grade provides information about the quality of the product, whereas the PG grade classifies the product according to the ASTM D 8239/21 [33] specification. In general, the addition of LNC in very small amounts increased one high-temperature PG grade for the neat asphalt cements and one or two for the SBS-modified binders. The LNC addition did not reduce the low-temperature PG grade, but such reduction was observed in the low-temperature PG continuous for several modified AC1 and AC2. A slight reduction in the low-temperature PG continuous grade was observed for the SBS-modified asphalt. The effects of the LNC on the continuous PG grade and on the PG grade were similar to those reported in the literature for graphene and graphene-oxide modified asphalts [3, 6, 34].

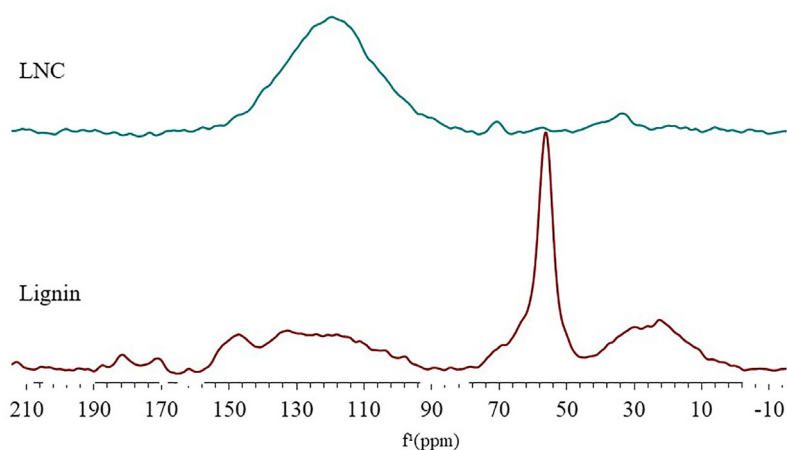


Figure 4: Comparison of <sup>13</sup>C DP/MAS.

**Table 4:** PG grade and PG continuous for the binders evaluated.

ASPHALT BINDER	PG GRADE	PG CONTINUOUS
AC1	64–22	66.3–22.7
AC110	70–22	71.9–22.9
AC1075	70–22	72.5–21.8
AC105	70–22	72.3–23.3
AC101	70–22	72.2–24.4
AC1005	70–16	72.2–23.5
AC1002	64–16	68.6–20.7
AC2	64–16	67.0–21.1
AC201	76–16	69.9–19.9
AC2005	76–16	76.0–20.9
SBS	76–22	77.6–28.3
SBS005	82–22	89.1–23.9
SBS002	88–22	87.6–27.5

**Table 5:** Effect of LNC modified asphalts on rutting.

SAMPLE ASPHALT BINDER	MSCR AT 64°C		BTSV	
	J <sub>n</sub> , 1/KPA	ELASTIC RECOVERY, %	T, °C	ä, °
AC1	3.48	0.63	43.37	78.22
AC110	1.33	2.86	55.21	81.27
AC1075	1.23	–	56.98	81.69
AC105	1.29	2.97	56.41	81.21
AC101	1.31	2.74	55.37	80.87
AC1005	1.27	–	55.41	81,30
AC1002	1.33	–	57.57	81,84
AC2	1.97	2.90	52.35	84.31
AC201	0.68	6.28	58.45	81.23
AC2005	0.64	6.97	58.45	81.20
SBS	0.38	46.56	54.55	70.20
SBS005	0.03	78.40	63.62	61.68
SBS002	0.04	77.01	62.56	62.66

### 3.2.2. Rutting resistance

Table 5 presents the results for the MSCR and BTSV parameters, related to rutting resistance. As shown, the non-recovery compliance decreased, and the elastic recovery increased with the LNC modification. The LNC addition to the SBS-modified binder increased the elastic recovery in more than 55%, decreased the BTSV temperature, and decreased the phase angle.

Figure 5 shows that the LNC modified asphalts derived from AC1 (Pen 50/70) and AC2 (Pen 30/45) behaved differently from SBS modified binder. Its BTSV temperature increased, and its phase angle remained in the same range of approximately 80° to 81°. The SBS and AC2 LNC modified products moved down and to the right, while the AC1 LNC modified products moved up and to the right side. The lower part of the graphic refers to more elastic responses, while the right part indicates a stiffer behavior. This results in a superior rutting resistance for the materials placed in that region of the plot. The benefits of rutting shown by the improvement of J<sub>n</sub> values was also verified in the literature for graphene derivatives [5, 34].

According to the MSCR results, the addition of LNC improved the rutting resistance, represented by the change from standard (S) to heavy (H) traffic level for the neat asphalt cements and from H to extremely heavy

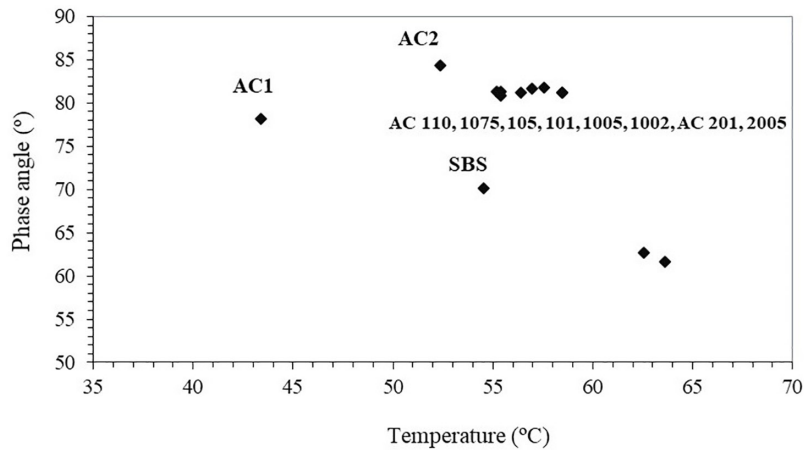


**Figure 5:** BTSV chart showing the position change of phase angle and temperature with LNC addition.

**Table 6:** Effect of LNC on the binder fatigue resistance.

SAMPLES	LAS FFL-PSE	$\Delta T_c$	R 9-59
AC1	1.55	1.94	1.88
AC110	1.61	0.35	1.87
AC1075	1.67	-0.45	-
AC105	1.62	-0.18	1.82
AC101	1.62	1.06	1.81
AC1005	1.63	0.1	-
AC1002	1.62	5.23	-
AC2	1.69	-0.16	2.00
AC201	1.81	-1.78	2.08
AC2005	1.76	-1.08	1.93
SBS	1.70	-0.66	2.19
SBS005	2.03	-4.61	2.58
SBS002	1.88	-0.99	2.14

(E) for the SBS-modified asphalts. This was followed with an increase of BTSV temperature, placing the samples on another position regarding the rutting resistance. The definitions of the designations S, H, V, and E are as follows (ASTM D8239/21) [33]:

- a) Standard Traffic, S, corresponds to traffic levels smaller than 10 million Equivalent Single-Axle Loads (ESALs) and traffic speeds higher than 70 km/h.  $J_{nr}$  should be between 4.5 and 2.0;
- b) Heavy Traffic, H, corresponds to traffic levels of 10 million to 30 million ESALs or slow-moving traffic (20 km/h to 70 km/h).  $J_{nr}$  should be between 2.0 and 1.0;
- c) Very Heavy Traffic, V, corresponds to traffic levels above 30 million ESALs or standing traffic (< 20 km/h).  $J_{nr}$  should be between 1.0 and 0.5;
- d) Extremely Heavy Traffic, E, corresponds to traffic levels above 30 million ESALs and standing traffic.  $J_{nr}$  should be less than 0.5.

### 3.2.3. Fatigue resistance

Table 6 shows the cracking-related parameters, i.e., FFL-PSE obtained from the LAS test,  $\Delta T_c$  and R value obtained from BBR test results. The LNC addition to asphalt cements increased FFL-PSE values indicating the enhancement of the fatigue resistance. On the other hand, no significant effects were observed on  $\Delta T_c$  and

R value. For the SBS-modified asphalt, FFL increased with the LNC modification. However, the use of 0.05% of LNC resulted in poor results for  $\Delta T_c$  and R value, placing them apart from the acceptable limits, presented on item 3.1. In contrast, the use of 0.02% of LNC produced very good results for  $\Delta T_c$  and R value.

### 3.2.4. Aging

The effects on aging were assessed based on  $|G^*|$  at 15°C and 10Hz, on the British specification parameter,  $|G^*|_{Tintermediate}$ , on the South African specification aging parameter, as presented in Table 7. In the analysis, the virgin and RTFOT + PAV aging states were considered.

The results showed that LNC improved the material aging resistance for asphalt cements as SBS modified asphalt. The aging indexes reduced after LNC addition for neat and SBS asphalt binders, both for  $|G^*|$  at 15°C and for  $|G^*|_{SA}$ . This effect has been reported in the literature for graphene [5]. LNC is a nanocarbon derived from lignin that holds anti-aging properties inherent to graphene derivatives (graphene oxide and reduced graphene oxide) [35].

### 3.2.5. Comparison of LNC modified asphalts with SBS-modified asphalts

Commercial SBS-modified asphalts (55/75) normally contain between 3.0% and 3.5% of SBS. As shown in Table 8, the addition of LNC to the SBS-modified binder (SBS) evaluated in the study resulted in material SBS002, with properties like those of the materials produced with higher concentrations of SBS.

For fatigue, the higher LAS FFL result indicated that SBS002 behaved better than HiMA (Highly-Modified Asphalt) and 60/85, which contained 7.5 and 5.0% of SBS, respectively. For rutting, SBS002 presented the same  $J_{nr}$  as HiMA and performed better than the 60/85, both for  $J_{nr}$  and Rec. The same PG grade was identified for these three materials. The same R values were obtained for SBS002 and HiMA. The analysis of the BTSV chart of Figure 6 indicates that SBS002 and HiMA presented a similar low phase angle, which results in a desirable more elastic behavior. In addition, the fact that SBS002 is positioned on the right in the chart infers that the material presented a higher stiffness.

**Table 7:** Aging indexes of LNC-modified asphalts in comparison with ACs and SBS-modified asphalts.

Sample	$ G^* $ at 15°C (PAV/VG)	$ G^* _{SA}$ (PAV/VG)
AC1	1.72	3.64
AC110	1.30	2.01
AC1075	1.40	2.21
AC105	1.26	2.37
AC101	1.26	2.5
AC1005	1.51	2.97
AC1002	1.24	2.31
AC2	1.53	3.37
AC201	1.38	2.11
AC2005	1.19	2.39
SBS	1.70	2.73
SBS002	1.23	2.42

**Table 8:** Properties of the SBS – modified asphalts.

TEST	SBS	SBS002	60/85	HiMA
LAS FFL RTFOT	1.45	1.89	1.55	1.65
$J_{nr}$ 64°C, 1/kPa	0.62	0.04	0.34	0.04
Rec, %	51.1	77.0	73.8	93.6
R – NCHRP	1.98	2.14	1.91	2.14
PG	64V-22	64E-22	64E-22	64E-22
BTSV – T, °C	54.55	62.56	51.64	49.49
BTSV – ä, °	70.20	62.66	68.28	64.15

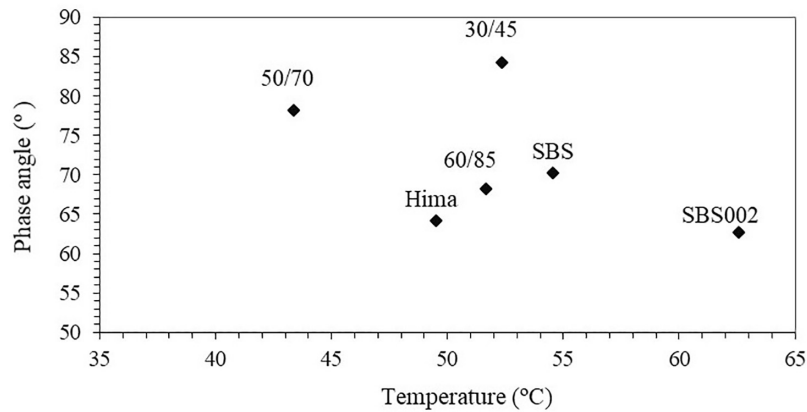


**Figure 6:** BTSV chart for the binders evaluated in the study.

**Table 9:** Storage stability of SBS modified asphalts.

SAMPLE	SOFTENING POINT TOP	SOFTENING POINT BOTTOM	DIFFERENCE
AC110	56.0	52.0	4.0
AC1005	54.0	50.0	4.0
AC2005	55.0	51.5	3.5
SBS	58.5	55.0	3.5
SBS002	60.0	58.0	2.0

### 3.2.6. Storage stability

It is important to know if LNC can compromise the storage stability of modified asphalt. This was evaluated following the procedures by ASTM D 7173/20 [36]. Table 9 presents the softening point (SP) values at the top and bottom of the tube left for 48 hours in an oven at 160°C. The differences obtained between the top and bottom results were smaller than the specified limit of 5°C for all materials.

## 4. SUMMARY AND CONCLUSIONS

This study characterized asphalt binders modified with lignin nanocarbon (LNC). Given its origin from lignin, LNC is regarded as a sustainable product that can be used in very small quantities as asphalt binder modifiers. The base materials were two neat binders, Pen 30/45 and Pen 50/70, and an SBS-modified binder (55/75). LNC was added in very small amounts (0.02% to 0.05%, w/w). LNC was characterized by NMR, elemental analysis, thermogravimetry, and x-ray diffraction. The chemical results showed that it seems to be very similar to reduced graphene oxide. Furthermore, the effects of the presence of the delocalized  $\pi$  electrons should be pronounced as the material becomes structurally more ordered in aromatic planes arranged in graphite-like micro-crystallites, which makes LNC a good candidate to act as an asphalt modifier.

The results of LNC modified asphalts obtained by rheological analysis led to the followings conclusions:

- The high-temperature PG of LNC-modified binders increased at least one grade for all samples in comparison to the base materials, meaning an increase in rutting performance;
- The superior rutting resistance was also confirmed by an upgrade of at least one traffic grade, considering the  $J_{nr}$  value obtained from the Superpave MSCR result analysis;
- The fatigue resistance was improved for all LNC-modified samples, considering the high values of FFL-PSE obtained from the LAS tests. In general, when a modifier provides the enhancement in rutting resistance, it may compromise the fatigue life. However, the resistance to both distresses was improved with the LNC incorporation;
- The LNC-modified asphalts presented better aging resistance than the neat and SBS-modified asphalts. This may result from a steric hindering to oxidation potentially promoted by LNC. This expected for nanostructures like graphene. In this research, the modifier was originated from lignin;

- The use of only 0.02% of LNC in the commercial SBS-modified binder resulted in the best combination, revealing a synergistic effect between the polymer and the nanocarbon, which behaved similarly or better than products with higher SBS concentrations, including HiMA.
- The oxygenated functional groups of LNC presented the advantage to allow the nanocarbon modifier to be reactive and compatible with the SBS copolymer. The performance improvements can be attributed to an increase in the crosslinking degree of the binders induced by the LNC. This has already occurred for similar nanocarbons from graphite.
- All LNC-modified asphalts presented good storage stability.

Declaration of competing interest.

The authors declare that there is no conflict of interest.

## 5. ACKNOWLEDGMENTS

This study was financed by the Coordination for the Improvement of Higher Education Personnel – Brazil (CAPES) – Financing Code 001 and by the National Council for Scientific and Technological Development (CNPq). The authors also thank the technical support from Alessandra Rangel Cassella (TGA and elemental analysis experiments), from the Brazilian National Institute of Metrology, Quality, and Technology (INMETRO), and from CENPES/PETROBRAS.

## 6. BIBLIOGRAPHY

- [1] ZHAO, Y., WEN, M., HE, C., *et al.*, “Preparation of graphene by catalytic pyrolysis of lignin and its electrochemical properties”, *Materials Letters*, v. 274, n. pp. 128047, 2020. <http://doi.org/10.1016/j.matlet.2020.128047>.
- [2] HILDE, S., XIAOHU, L., UWE, M., *et al.*, “Influence of aging on binder fatigue and other fracture related binder test results”, In: International Society for Asphalt Pavements Conference – ISAP 2016, Symposium Jackson Hole, Wyoming, USA, 2016.
- [3] MADURANI, K.A., SUPRAPTO, S., MACHRITA, N.I., *et al.*, “Progress in graphene synthesis and its application: history, challenge and the future outlook for research and industry”, *ECS Journal of Solid State Science and Technology*, v. 9, pp. 093013, 2020. doi: <http://doi.org/10.1149/2162-8777/abbb6f>.
- [4] POLO-MENDOZA, R., NAVARRO-DONADO, T., ORTEGA-MARTINEZ, D., *et al.*, “Properties and characterization techniques of graphene modified asphalt binders”, *Nanomaterials (Basel, Switzerland)*, v. 13, n. 955, pp. 955, 2023. doi: <http://doi.org/10.3390/nano13050955>. PubMed PMID: 36903833.
- [5] ASIM, N., BADIEI, M., SAMSUDIN, N.A., *et al.*, “Application of graphene-based materials in developing sustainable infrastructure: an overview”, *Composites. Part B, Engineering*, v. 245, pp. 110188, 2022. doi: <http://doi.org/10.1016/j.compositesb.2022.110188>.
- [6] HE, J., HU, W., XIAO, R., *et al.*, “Review on graphene/GNPs/GO modified asphalt”, *Construction & Building Materials*, v. 330, pp. 127222, 2022. doi: <http://doi.org/10.1016/j.conbuildmat.2022.127222>.
- [7] MORENO-NAVARRO, F., SOL-SÁNCHEZ, M., GÁMIZ, F., *et al.*, “Mechanical and thermal properties of graphene modified asphalt binders”, *Construction & Building Materials*, v. 180, pp. 265–274, 2018. doi: <http://doi.org/10.1016/j.conbuildmat.2018.05.259>.
- [8] YAO, H., WANG, Y., LIU, J., *et al.*, “Review on applications of lignin in pavement engineering: a recent survey”, *Frontiers in Materials*, v. 8, pp. 803524, 2022. doi: <http://doi.org/10.3389/fmats.2021.803524>.
- [9] WEI, Y., LIU, Y., MUHAMMAD, Y., *et al.*, “Study on the properties of GNPs/PS and GNPs/ODA composites incorporated SBS modified asphalt after short-term and long-term aging”, *Construction & Building Materials*, v. 261, pp. 119682, 2020. doi: <https://doi.org/10.1016/j.conbuildmat.2020.119682>.
- [10] HAN, M., MUHAMMAD, Y., WEI, Y., *et al.*, “A review on the development and application of graphene-based materials for the fabrication of modified asphalt and cement”, *Construction & Building Materials*, v. 285, pp. 122885, 2021. doi: <http://doi.org/10.1016/j.conbuildmat.2021.122885>.
- [11] ROCHA, D., LUZARDO, J., AGUIAR, D., *et al.*, “Towards an enhanced nanocarbon crystallization from lignin”, *Carbon*, v. 203, pp. 120–129, 2023. doi: <http://doi.org/10.1016/j.carbon.2022.11.036>.
- [12] HABIB, N.Z., AUN, N.C., ZOOROB, S.E., *et al.*, “Use of graphene oxide as a bitumen modifier: an innovative process optimization study”, *Advanced Materials Research*, v. 1105, pp. 365–369, 2015. doi: <http://doi.org/10.4028/www.scientific.net/AMR.1105.365>.

- [13] LIU, K., ZHANG, K., SHI, X., “*Performance evaluation and modification mechanism analysis of asphalt*”, *Construction & Building Materials*, v. 163, pp. 880–889, 2018. doi: <http://doi.org/10.1016/j.conbuildmat.2017.12.171>.
- [14] LI, Z., CHEN, W., LI, Y., *et al.*, “*Characteristic evolution of GO/SBS-modified asphalt during aging*”, *Advances in Civil Engineering*, v. 2022, pp. 4060013, 2022. doi: <https://doi.org/10.1155/2022/4060013>.
- [15] AMERICAN SOCIETY FOR TESTING AND MATERIALS, *ASTM D7405/20 Standard Practice for Multiple Stress Creep and Recovery (MSCR) of Asphalt Binder Using a Dynamic Shear Rheometer*, ASTM, 2020.
- [16] AMERICAN ASSOCIATION OF STATE AND HIGHWAY TRANSPORTATION OFFICIALS, *AASHTO T 391/20 Standard Method of Test for Estimating Fatigue Resistance of Asphalt Binders Using the Linear Amplitude Sweep*, AASHTO, 2020.
- [17] AMERICAN ASSOCIATION OF STATE AND HIGHWAY TRANSPORTATION OFFICIALS, *AASHTO PP 78/17 Standard Practice for Design Considerations Ehen Using Reclaimed Asphalt Shingles (RAS) in Asphalt Mixtures*, AASHTO PP78.
- [18] DEUTSCHES INSTITUT FUR NORMUNG, *DIN 52050 Bitumen und bitumenhaltige Bindemittel – BTSV – Prüfung*. Deutsches Institut für Normung e. V. Beuth Verlag, 20218, DIN.
- [19] AMERICAN SOCIETY FOR TESTING AND MATERIALS, *ASTM D 7643/22 Standard Practice for Determining the Continuous Grading Temperatures and Continuous Grades for PG Graded Asphalt Binders*, West Conshohocken, ASTM, 2022.
- [20] NASCIMENTO, L.A.H., “*Implementation and validation of the viscoelastic continuum damage theory for asphalt mixture and pavement analysis in Brazil*”, Ph.D. Dissertation, North Carolina State University, Raleigh, NC, USA, 2014.
- [21] HINTZ, C., “*Understanding Mechanisms Leading to Asphalt Binder Fatigue*”, Ph.D. Dissertation, University of Wisconsin, Madison, WI, 2012.
- [22] UNDERWOOD, B.S., KIM, Y.R., “*Experimental investigation into the multiscale behaviour of asphalt concrete*”, *The International Journal of Pavement Engineering*, v. 12, n. 4, pp. 357–370, 2011. doi: <http://doi.org/10.1080/10298436.2011.574136>.
- [23] ASPHALT INSTITUTE, *Use of the Delta Tc Parameter to Characterize Asphalt Binder Behavior*, Asphalt Institute Technical Advisory Committee, New Westminster, 2019.
- [24] CHRISTENSEN, D.W., TRAM, N., *Relationships between the fatigue properties of asphalt binders and the fatigue performance of asphalt mixtures*, National Cooperative Highway Research Program, USA, 2022.
- [25] AMERICAN ASSOCIATION OF STATE AND HIGHWAY TRANSPORTATION OFFICIALS, *AASHTO M 320 “Performance – Graded Asphalt Binder”*, Standard Specifications for Transportation Materials and Methods of Sampling and Testing, 2010, AASHTO.
- [26] AMERICAN ASSOCIATION OF STATE AND HIGHWAY TRANSPORTATION OFFICIALS, *AASHTO T 315 Standard Method of Test for Determining the Rheological Properties of Asphalt Binder Using a Dynamic Shear Rheometer (DSR)*. American Association of State Highway and Transportation Officials, 2012, AASHTO.
- [27] BREDEHANN, S.J., MYBURGH, P.A., JENKINS, K.J., *et al.*, “*Implementation of a performance-grade bitumen specification in South Africa*”, *Journal of the South African Institution of Civil Engineering*, v. 61, n. 3, pp. 20–31, 2019. doi: <http://dx.doi.org/10.17159/2309-8775/2019/v61n3a3>.
- [28] SCHRADER, J., WISTUBA, M.P., FALCHETTO, A.C., *et al.*, “*A new binder-fast-characterization-test using a dynamic shear rheometer and its application for rejuvenating reclaimed asphalt binder*”, *Journal of Testing and Evaluation*, v. 48, n. 1, pp. 52–59, 2020. doi: <http://doi.org/10.1520/JTE20180893>.
- [29] BRITISH STANDARDS INSTITUTION, *Series 900, Specification for Highway works – Volume 1 – Road pavements – Bituminous Bound Materials*, British Standards Institution, Reino Unido, 2021.
- [30] GROSSMAN, A., VERMERRIS, W., “*Lignin-based polymers and nanomaterials*”, *Current Opinion in Biotechnology*, v. 56, pp. 112–120, 2019. doi: <http://doi.org/10.1016/j.copbio.2018.10.009>. PMID:30458357.
- [31] MAHAJAN, C.R., MISHRA, S., “*Effect of graphitic nanomaterials on thermal, mechanical and morphological properties of polypropylene nanocomposites*”, *Research & Development in Material Science*, vol. 11, no. 4, pp. 1190-1201, 2019. doi: <http://doi.org/10.31031/RDMS.2019.11.000766>.

- [32] SIONG, V.L.E., LEE, K.M., JUAN, J.C., *et al.*, “*Removal of methylene blue dye by solvothermally reduced graphene oxide: a metal-free adsorption and photodegradation method*”, RSC Advances, v. 9, n. 64, pp. 37686-37695, 2019. doi: <http://doi.org/10.1039/C9RA05793E>.
- [33] AMERICAN SOCIETY FOR TESTING AND MATERIALS, ASTM D 8239/21 Standard Specification for Performance – Graded Asphalt Binder Using the Multiple Stress Creep and Recovery, 2021, ASTM.
- [34] LI, B., LIU, P., ZHAO, Y., *et al.*, “*Effect of graphene oxide in different phases on the high temperature rheological properties of asphalt based on grey relational and principal component analysis*”, Construction & Building Materials, v. 362, pp. 129714, 2023. doi: <http://doi.org/10.1016/j.conbuildmat.2022.129714>.
- [35] WU, S., ZHAO, Z., LI, Y., *et al.*, “*Evaluation of aging resistance of graphene oxide modified asphalt*”, Applied Sciences (Basel, Switzerland), v. 7, n. 7, pp. 702, 2017. doi: <http://doi.org/10.3390/app7070702>.
- [36] ZHENGLONG, M., “*Study on the performance and aging low temperature performance of GO/SBS modified asphalt*”, Revista Matéria, vol. 28, n. 3, pp. e20230151, 2023. doi: <https://doi.org/10.1590/1517-7076-RMAT-2023-0151>.